Production of fast H^0 atoms by stripping H^- ions in gas and vapor targets

C. J. Anderson,* R. J. Girnius, A. M. Howald, and L. W. Anderson
Department of Physics, University of Wisconsin, Madison, Wisconsin 53706
(Received 27 November 1979)

Measurements of the total charge-changing cross sections σ_{-0} and σ_{-+}, are reported for H^- ions with energies in the range 30–200 keV incident on Ne, Ar, Kr, Xe, Li, Na, K, Rb, and Cs gas or vapor targets. Measurements of σ_{g+} and σ_{g-} are reported for fast ground-state H^0 atoms with energies of 30–200 keV incident on the same targets. Measurements are also reported on the fractional yields as a function of the target thickness for H^- ions with energies in the range 30–200 keV incident on a variety of targets. The neutral fraction increases, reaches a maximum value, F_0^{max}, and then decreases to the equilibrium fraction F_0^∞ as the target thickness increases from 0 to a very large value. Measurements of F_0^{max}, F_0^∞, and F_-^∞ are reported for H^- ions incident on a variety of targets.

I. INTRODUCTION

This paper reports measurements of cross sections and fractional yields important for understanding the production of fast H^0 or D^0 atoms by the collisional stripping of H^- or D^- ions, respectively. The production of fast D^0 atoms is important for the controlled thermonuclear research program. A promising method of heating a magnetically confined plasma is by the injection of an intense beam of fast D^0 atoms into the plasma. One method of producing a beam of fast D^0 atoms is (i) form a beam of D^- ions at low energy, (ii) accelerate the D^- ions to a high energy, and (iii) strip an electron off the fast D^- ions thereby forming fast D^0 atoms. In the energy range 30–200 keV the total charge-changing cross sections and fractional yields are the same for either deuterium ions or atoms and hydrogen ions or atoms incident on a target at the same velocity (see Sec. III of this paper). For most of our measurements we use fast H^- ions or H^0 atoms incident rather than D^- ions or D^0 atoms. We report measurements of σ_{-0} and σ_{-+} for H^- incident at 30–200 keV on Ne, Ar, Kr, Xe, Li, Na, K, Rb, and Cs gas or vapor targets, where σ_{-0} and σ_{-+} are, respectively, the total charge-changing cross sections to strip one and two electrons from a H^- ion. We also report measurements of σ_{g+} and σ_{g-} for fast ground-state H^0 atoms incident at 30–200 keV on the same targets where σ_{g+} and σ_{g-} are, respectively, the total charge-changing cross sections to strip an electron from a fast ground-state H^0 atom and to form a H^- ion from a fast ground-state H^0 atom. We have also measured the fractional yields as a function of the target thickness, π, in atoms/cm^2 when H^- ions are incident with an energy of 30–200 keV on a variety of gas or vapor targets. As a function of π the neutral fraction F_0 is found to increase from $F_0 = 0$ at $\pi = 0$, reach a maximum F_0^{max}, and then decrease becoming constant at the equilibrium fraction F_0^∞, at very large values of π. We report measurements of F_0^{max} when H^- ions are incident with an energy of 30–200 keV on the following gas or vapor targets: H_2, D_2, He, Ne, Ar, Kr, Xe, Li, Na, K, Rb, Cs, N_2, O_2, CO_2, SF_6, C_4H_{10}, C_5H_{12}, Br_2, I_2, CF_4, CHF_3, $CBrF_3$, H_2O, acetone, 2-propanal, and natural gas. We also report measurements of the neutral and negative equilibrium fractions F_0^∞ and F_-^∞, for 30–200 keV H^- ions in-

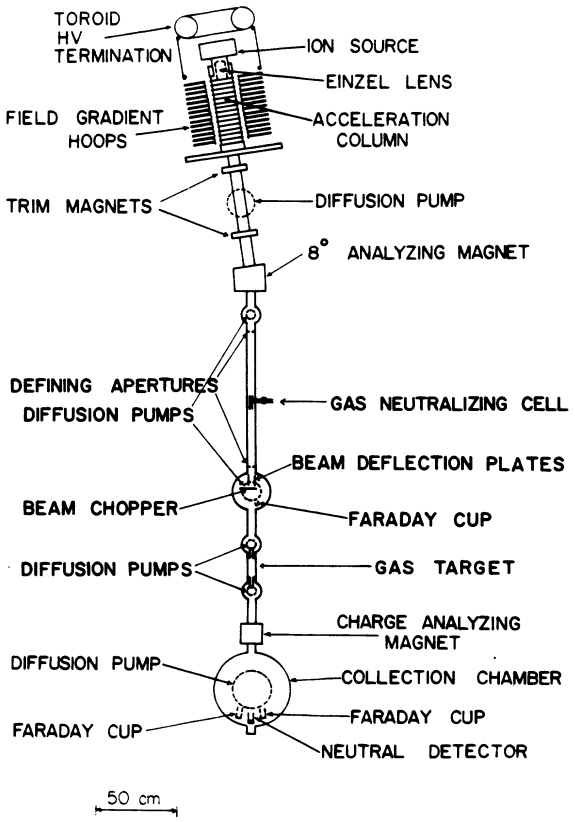

FIG. 1. Schematic diagram of the apparatus.

TABLE I. Total cross section σ_{-0} (10^{-17} cm^2) for H^- or D^- ions incident on He, Ne, Ar, Kr, and Xe as a function of beam energy (keV).

Ion	Energy (keV)	He	Ne	Ar	Kr	Xe
H^-	50	32	47 ± 5	121 ± 12	141 ± 14	177 ± 18
	75	27	45 ± 5	97 ± 10	123 ± 12	125 ± 13
	100	22	42.3 ± 4	88.4 ± 9	115 ± 11	113 ± 11
	150	18	37.5 ± 4	79.0 ± 8	98 ± 10	99 ± 10
	200	15	35.0 ± 4	68.5 ± 7	88 ± 9	90 ± 9
D^-	50		47.5 ± 5	141 ± 15		218 ± 22
	100		47.1 ± 5	118 ± 12		173 ± 17
	150		45.7 ± 5	99 ± 10		
	200		43.3 ± 4	91 ± 9		

cident on the following gas or vapor targets: H_2, He, Ne, Ar, Kr, Xe, Li, Na, K, Rb, and Cs. The measured values of F_0^{max} and F_0^{∞} are compared with calculated values of these quantities based on a three-component model using experimental values for the various cross sections.

II. APPARATUS

A schematic diagram of our apparatus is shown in Fig. 1. The accelerator produces a beam of singly charged ions in the energy range 30–200 keV. Direct extraction from a duoplasmatron ion source with an offset anode is used to produce a H^- ion beam. The beam is extracted using a Pierce geometry. It is momentum analyzed and then collimated by two 1.5-mm apertures 90 cm apart. Located between the apertures is a gas neutralizing target. Following the collimation section, the ion beam passes between two parallel plates to which a voltage can be applied. The proper electric field between the plates deflects the beam into a suppressed Faraday cup located off the beam axis. This cup measures the incident negative ion beam. When the plates are grounded, the negative ion beam passes through them entering the target. The beam is chopped mechanically at 5 Hz before it enters the target.

Two different targets were used, one for gases and one for alkali metal vapors. The gas target is 15.3 cm long. The gas flow from the target is reduced by using 7.4-mm-i.d. tubes 8.78 cm long for the entrance and exit apertures of the target. The pressure in the target is measured with an RCA-1949 ionization gauge. The ionization gauge was calibrated for each gas with a MKS Baratron capacitance manometer. The capacitance manometer was checked against a calibrated Wallace and Tiernan gauge. We estimate the uncertainty in the pressure measurement is ±8%.

The alkali metal target is made of stainless steel and is 16.5 cm long and 2.54 cm i.d. The metal vapor flow from the target is reduced by using 6.4-mm-i.d. tubes 5.1 cm long for exit and entrance apertures. The alkali metal reservoir is

TABLE II. Total cross section σ_{-0} (10^{-17} cm^2) for H^- ions incident on Li, Na, K, Rb, and Cs as a function of beam energy (keV).

Energy (keV)	Li	Na	K	Rb	Cs
30	140 ± 28	145 ± 29	249 ± 50	263 ± 53	284 ± 29
40	125 ± 16	133 ± 27	219 ± 44	248 ± 50	247 ± 27
50	119 ± 24	130 ± 26	205 ± 41	233 ± 47	228 ± 23
60	115 ± 23	127 ± 25	195 ± 40	215 ± 44	220 ± 22
75					209 ± 21
80	105 ± 21	120 ± 24	178 ± 36	200 ± 40	
100	96 ± 19	112 ± 22	157 ± 31	188 ± 38	180 ± 18
140					157 ± 16
150	78 ± 16	98 ± 20	146 ± 29	170 ± 34	
180					145 ± 17
200	71 ± 15	84 ± 17	133 ± 27	150 ± 31	135 ± 16

TABLE III. Total cross section σ_{-+} (10^{-18} cm^2) for H^- or D^- ions incident on He, Ne, Ar, Kr, and Xe as a function of beam energy (keV).

Ion	Energy (keV)	He	Ne	Ar	Kr	Xe
H^-	50	23	67.3 ± 7	212 ± 21	179 ± 18	235 ± 24
	75	17	65.9 ± 7	194 ± 20	153 ± 15	201 ± 20
	100	12	65.6 ± 7	160 ± 16	128 ± 13	138 ± 14
	150	8.0	50.5 ± 5	121 ± 12	113 ± 11	106 ± 11
	200	6.2	41.5 ± 4	97 ± 10	105 ± 11	97 ± 10
D^-	50		58.0 ± 6	201 ± 20		183 ± 18
	100		69.8 ± 7	226 ± 23		239 ± 24
	150		65.2 ± 7	201 ± 20		
	200		60.3 ± 6	171 ± 17		

located directly below the target and is connected to the target by a 1.9-cm-i.d. tube. The level of the alkali metal surface is about 2.5 cm below the target chamber. The target chamber is kept at least 150°C above the highest reservoir temperature used during the cross section measurements. Condensation of the alkali metal in the target chamber is thus avoided. The reservoir temperature determines the alkali metal vapor pressure above the alkali metal surface. The alkali metal vapor pressure in the target is about (6–8%) less than the pressure immediately above the molten liquid due to the conductance of the various tubes. The alkali metal vapor pressure in the target is determined from measurements of the temperature of the alkali metal in the reservoir using the known temperature dependence of the vapor pressure of the alkali metal[1] and using the calculated conductance of the tube from the molten alkali to the target, the conductance of the target, and the conductance of the entrance and exit tubes. A stainless steel-clad iron-constantan thermocouple inserted into the molten alkali metal measures the temperature of the alkali metal. As a check of the accuracy of the iron-constantan thermocouple we have measured the melting points of the alkali metals and find the measured melting points are less than 0.5°C from the accepted melting points in all cases. Error in the measurements of the alkali metal vapor pressure can result from (i) uncertainties in the vapor pressure versus temperature measurements (~15%), (ii) the surface of the liquid metal being a slightly different temperature than the interior of the liquid metal (~10%), (iii) contamination of the liquid metal surfaces, and (iv) random errors in temperature measurement, etc. (~5%). Our estimate of the total uncertainty in the measurement of the alkali metal vapor pressure is about ±25%.

The beam emerging from the target is composed of positive and negative ions as well as fast neutral atoms. This beam is separated into its charge states by a magnet that deflects the positive and negative ions into two suppressed Faraday cups located symmetrically at ±4% to the left and right of the beam axis. The neutral beam emerging from the target is undeflected and strikes a pyro-

TABLE IV. Total cross section σ_{-+} (10^{-18} cm^2) for H^- ions incident on Li, Na, K, Rb, and Cs as a function of beam energy (keV).

Energy (keV)	Li	Na	K	Rb	Cs
30	68 ± 14	62 ± 12	272 ± 54	275 ± 56	223 ± 22
40	65 ± 13	67 ± 13	283 ± 57	290 ± 58	235 ± 24
50	63 ± 13	70 ± 14	311 ± 62	280 ± 56	234 ± 24
60	60 ± 12	71 ± 14	291 ± 58	250 ± 50	208 ± 21
75					177 ± 18
80	56 ± 11	71 ± 14	264 ± 53	230 ± 46	
100	51 ± 10	69 ± 14	220 ± 44	215 ± 43	130 ± 13
140					100 ± 10
150	37 ± 8	65 ± 13	179 ± 36	190 ± 38	
180					89 ± 11
200	27 ± 6	62 ± 13	157 ± 32	175 ± 36	84 ± 11

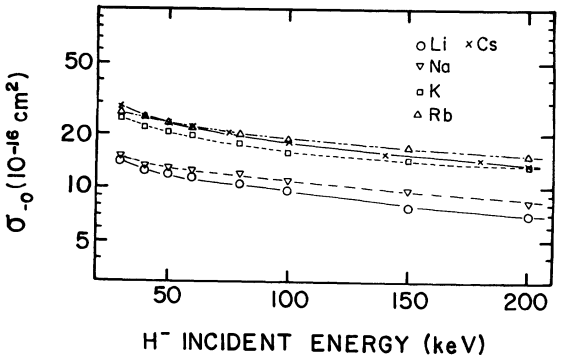

FIG. 2. σ_{-0} as a function of the energy for H^- ions incident on Li, Na, K, Rb, and Cs vapor targets.

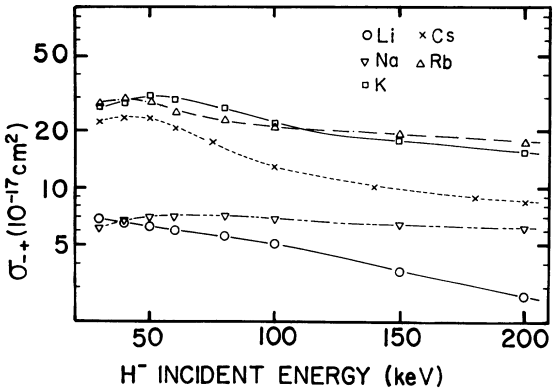

FIG. 3. σ_{-+} as a function of the energy for H^- ions incident on Li, Na, K, Rb, and Cs vapor targets.

electric crystal that measures the power in the neutral beam.[2,3] The calibration of the pyroelectric crystal has been described previously.[4] For some experiments the H^- ion beam is neutralized by the gas neutralizing target.

III. CROSS SECTION MEASUREMENTS

The experimental data, from which the cross sections are extracted, are measured values of N_+, N_-, N_0, N_s, and the target chamber pressure, where N_+, N_-, and N_0 are the measured number of positive, negative and neutral particles/sec emerging from the target, and where N_s is the number of particles/sec incident on the target. The total number of particles emerging from the target N_d is given by

$$N_d = N_+ + N_0 + N_- . \tag{1}$$

We define the transmission of the beam through the target as $T = N_d/N_s$. Particles can be lost from the beam due to misalignment, stray electric and magnetic fields, or scattering through angles large enough that the particles miss the detector. For measurements of the cross sections the measured value of T is greater than 0.99. Since $T > 0.99$ we conclude that various mechanisms that result in the loss of beam are not important in our measurements of cross sections. The fractional yields of H^+ ions (F_+), fast H^0 atoms (F_0), and H^- ions (F_-) are given by

$$F_+ = N_+/N_d \simeq N_+/N_s, \quad F_0 = N_0/N_d \simeq N_0/N_s, \quad F_- = N_-/N_d \simeq N_-/N_s . \tag{2}$$

It follows from Eqs. (1) and (2) that $F_+ + F_0 + F_- = 1$.

The important target parameter is the target thickness π, which is measured in particles/cm^2. The pressure outside the target is very low compared to the pressure inside the target. Therefore the gas target thickness π in atoms/cm^2 is given by $\pi = ln$ where l is the length of the target chamber plus $\frac{1}{2}$ the length of the entrance tube, plus $\frac{1}{2}$ the length of the exit tube, and where n is the target density in atoms/cm^3. The target density n is derived from the gas or vapor pressure in the target using the ideal-gas law.

The cross sections σ_{-0} and σ_{-+} are measured as follows. A beam of H^- ions is incident on the target. From the measured values of N_+, N_0, N_-, and N_s as functions of π we obtain F_+, F_-, and F_0 as functions of π. At very small values of target thickness the fractions of the beam emerging from the target are given by

$$F_+ = \sigma_{-+}\pi = N_+/N_d \simeq N_+/N_s, \quad F_0 = \sigma_{-0}\pi = N_0/N_d \simeq N_0/N_s, \tag{3}$$

and

$$F_- = 1 - (\sigma_{-+} + \sigma_{-0})\pi = N_-/N_d \simeq N_-/N_s .$$

At low values of π we find experimentally that F_-, F_0, and F_+ are all linear functions of π. The cross sections σ_{-+} and σ_{-0} are obtained, respectively,

TABLE V. Total cross section σ_{g+} (10^{-18} cm^2) for H_0 or D^0 atoms incident on He, Ne, Ar, Kr, and Xe as a function of beam energy (keV).

Ion	Energy (keV)	He	Ne	Ar	Kr	Xe
H^0	50	123	208 ± 21	442 ± 44	368 ± 37	535 ± 54
	75	108	207 ± 21	476 ± 48	385 ± 39	505 ± 51
	100	92	198 ± 20	420 ± 42	385 ± 39	455 ± 46
	150	72	189 ± 19	357 ± 36	360 ± 36	411 ± 41
	200	58	173 ± 17	343 ± 34	350 ± 35	376 ± 38
D^0	50		170 ± 17	366 ± 37		357 ± 36
	100		207 ± 21	464 ± 46		545 ± 55
	150		215 ± 22	460 ± 46		
	200		206 ± 21	430 ± 43		

TABLE VI. Total cross section σ_{g+} (10^{-18} cm^2) for H^0 atoms incident on Li, Na, K, Rb, and Cs as a function of beam energy (keV).

Energy (keV)	Li	Na	K	Rb	Cs
30	240 ± 50	200 ± 40	584 ± 120	600 ± 120	592 ± 60
40	250 ± 50	230 ± 45	622 ± 125	630 ± 125	639 ± 64
50	240 ± 50	260 ± 50	622 ± 125	640 ± 130	672 ± 67
60	240 ± 50	290 ± 60	611 ± 125	620 ± 125	648 ± 65
75					609 ± 61
80	230 ± 45	300 ± 60	583 ± 120	610 ± 120	
100	210 ± 40	290 ± 60	567 ± 115	595 ± 120	558 ± 60
140					465 ± 47
150	180 ± 40	270 ± 55	515 ± 110	565 ± 115	
170					423 ± 42
200	160 ± 35	250 ± 50	471 ± 100	550 ± 110	408 ± 41

from the slopes of F_+ and F_0 as functions of π. Our measurements of σ_{-0} and σ_{-+} as a function of the incident H^- ion energy are tabulated in Tables I–IV and some of our measurements are shown in Figs. 2 and 3. The values of σ_{-0} and σ_{-+} for Cs and He targets are from Refs. 4 and 5, respectively.

The uncertainties in the measurements of σ_{-0} and σ_{-+} result from random scatter in the measurements and from the uncertainty in the measurements of the target density. The absolute uncertainty for the inert-gas cross sections are generally about ±10%. The absolute uncertainty for the alkali metal cross sections is estimated to be about ±25% due to the larger uncertainty in measuring the target density. The relative uncertainty for cross sections with the same target is estimated to be less than ±10%.

The cross sections σ_{g+} and σ_{g-} are measured as follows. A beam of fast H^0 atoms is incident on the target. The beam of fast H^0 atoms is prepared by passing H^- ions through an Ar gas target. Any H^+ and H^- ions remaining in the beam after the Ar target are removed using the electrostatic deflection plates. The electric field between the deflection plates also quenches any metastable H(2s) atoms formed either directly or by cascading. The flight time from the gas neutralizing target to the deflection plates is long compared to the radiative lifetime of an H^0 atom with $n \lesssim 6$. Thus most of the H^0 atoms are in the ground state. From the measured values of N_+, N_0, and N_- as functions of π, we obtain the fractions F_+, F_0, and F_-, as functions of π. At very low target thickness the fractions as a function of π are given by

$$F_+ = \sigma_{g+}\pi = N_+/N_g \simeq N_+/N_s ,$$

$$F_0 = 1 - (\sigma_{g+} + \sigma_{g-})\pi = N_0/N_g \simeq N_0/N_s ,$$

and

$$F_- = \sigma_{g-}\pi = N_-/N_g \simeq N_-/N_s .$$

TABLE VII. Total cross section σ_{g-} (10^{-20} cm^2) for H^0 or D^0 atoms incident on He, Ne, Ar, Kr, and Xe as a function of beam energy (keV).

Ion	Energy (keV)	He	Ne	Ar	Kr	Xe
H^0	50	470	509 ± 70	530 ± 72	836 ± 92	778 ± 92
	75	270	344 ± 47	320 ± 46	470 ± 60	590 ± 70
	100	130	210 ± 30	195 ± 29	241 ± 35	345 ± 46
	150	50	122 ± 18	74 ± 11	77 ± 12	107 ± 15
	200	23	67 ± 10	33 ± 6	30 ± 5	47 ± 7
D^0	50		858 ± 90	1070 ± 100		3450 ± 350
	100		508 ± 70	518 ± 72		777 ± 90
	150		348 ± 50	307 ± 45		
	200		222 ± 33	198 ± 30		

TABLE VIII. Total cross section σ_{g-} (10^{-20} cm^2) for H^0 atoms incident on Li, Na, K, Rb, and Cs as a function of beam energy (keV).

Energy (keV)	Li	Na	K	Rb	Cs
30	170 ± 51	270 ± 70	541 ± 140	740 ± 190	910 ± 137
40	90 ± 27	180 ± 45	497 ± 125	540 ± 135	776 ± 116
50	70 ± 21	160 ± 40	393 ± 99	440 ± 110	679 ± 100
60	62 ± 19	150 ± 38	314 ± 79	330 ± 83	642 ± 96
75					482 ± 72
80	49 ± 16	140 ± 35	201 ± 51	250 ± 63	
100	41 ± 13	120 ± 30	157 ± 40	195 ± 49	375 ± 56
140					191 ± 29
150		68 ± 17	76 ± 19		
170					93 ± 19
200		52 ± 14	35 ± 9		

At low values of π we find experimentally that the fractions F_0, F_+, and F_- are all linear functions of π. The cross sections σ_{g+} and σ_{g-} are obtained from the slopes of F_+ and F_- as functions of π. Our measurements of σ_{g+} and σ_{g-} are tabulated in Tables V–VIII and some of our measurements are shown in Figs. 4 and 5. The values of σ_{g+} and σ_{g-} for Cs and He targets are from Refs. 1 and 9, respectively. The uncertainty in σ_{g+} is ±10% for the inert gases and ±25% for the alkali metals. The uncertainty in σ_{g-} is ±20% for the inert gases and ±30% for the alkali metals. There is a larger uncertainty in the cross section σ_{g-} than in σ_{g+} because the small negative ion currents from which σ_{g-} is obtained have a larger random scatter than is present in most the other measurements.

Tables I, III, V, and VII present the cross sections σ_{-0}, σ_{-+}, σ_{g+}, and σ_{g-} for both hydrogen and deuterium incident on Ne, Ar, and Kr. Shown in Fig. 6 are the cross sections σ_{-0}, σ_{-+}, and σ_{g+} for both hydrogen and deuterium incident on Ne. The deuterium data are plotted at half the incident energy so that it is plotted at the same velocity as the hydrogen data. As shown in Tables I, III, V, and VII and Fig. 6 the cross sections σ_{-0}, σ_{-+}, σ_{g+} and σ_{g-} for hydrogen and deuterium incident on Ne, Ar, and Xe are indistinguishable within experimental uncertainty when the deuterium and hydrogen have the same incident velocity. Other experiments we have carried out indicate that the cross sections and fractional yields are identical when hydrogen or deuterium ions or atoms are incident on a target with the same velocity in the energy range 30–200 keV for incident H^+ ions.

There have been some previous measurements by others of some of the cross sections that we have measured.[6-17] Table IX presents a brief comparison of our measurements and the measurements of others. Our measurements of σ_{g+} may differ from measurements of σ_{g+} by others in that our fast neutral beam was prepared by stripping an H^- ion beam, whereas others have pre-

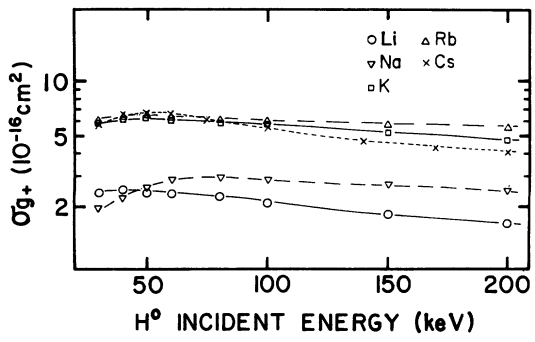

FIG. 4. σ_{g+} as a function of the energy for fast ground-state H^0 atoms incident on Li, Na, K. Rb, and Cs vapor targets.

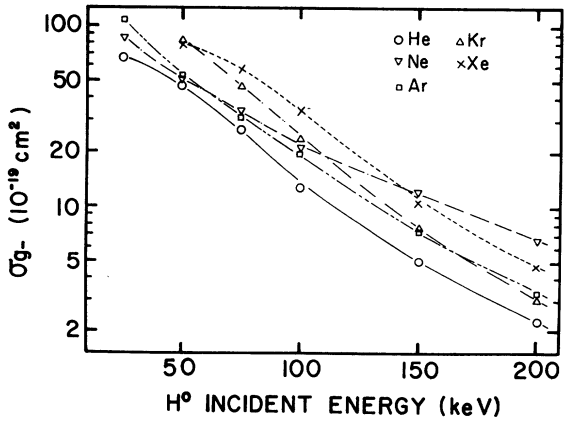

FIG. 5. σ_{g-} as a function of the energy for fast ground-state H^0 atoms incident on He, Ne, Ar, Kr, and Xe targets.

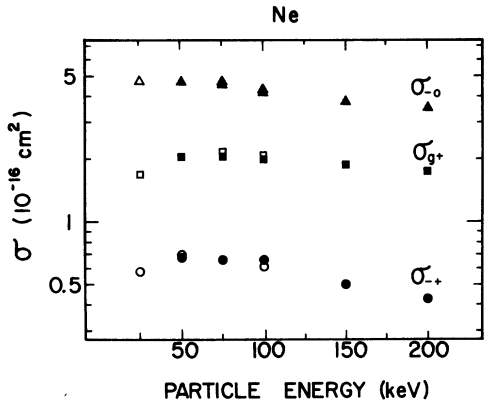

FIG. 6. σ_{-0}, σ_{g+}, and σ_{-+} as a function of the energy for a Ne target. The open symbols are for D ions or atoms incident. The solid symbols are for H ions or atoms incident. The deuterium data are plotted at half the incident energy.

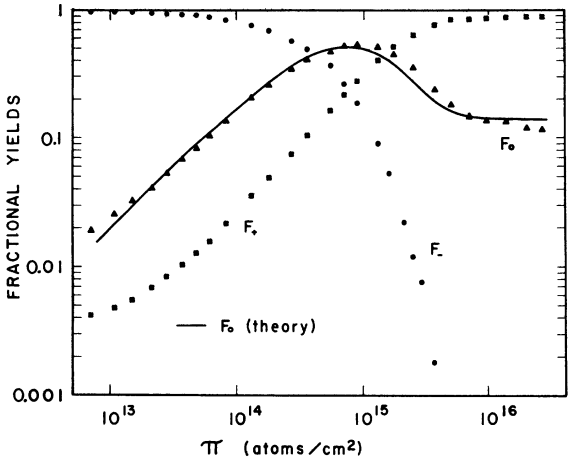

FIG. 7. F_+, F_0, and F_- as a function of the energy for H_- ions incident on a K target.

TABLE IX. Comparison of the previous measurements of σ_{-0}, σ_{-+}, σ_{0+}, and σ_{0-} by others with our measurements. For each cross section we show the authors, the reference, and the energy range of the previous measurements and the percentage difference between our measurements and the previous measurements. Thus our measured values for σ_{-0} are less than 10% higher than the previous measurements of Stier and Barnett in the energy range where the measurements overlap.

Reference		Energy (keV)	Ne	Ar	Kr	Xe	Li
σ_{-0}							
Stedeford and Hasted	Ref. 15	3–40	+15%	+15%	+110%	+100%	
Williams	Ref. 12	2–50	<15%	<15%	+80%	+40%	
Stier and Barnett	Ref. 6	3–40	<10%	<10%			
Heinemeier	Ref. 10	50–500		<5%			
Morgan *et al.*	Ref. 16	1.25–25				<5%	
σ_{-+}							
Fogel' *et al.*	Ref. 13	5–40	−10%	−20%	−30%	−20%	
Williams	Ref. 12	2–50	<5	−20%			
Heinemeier	Ref. 10	50–500		−15%			
Morgan *et al.*	Ref. 16	1.25–25				<5%	
σ_{0+}							
Stier and Barnett	Ref. 6	3–200	<10%	<10%			
Fogel' *et al.*	Ref. 14	5–40	−10%	−30%	−15%	−25%	
Solov'ev *et al.*	Ref. 8	10–180	−15%	+10%	+60%		
Williams	Ref. 11	2–50	<10%	<10%	+60%	+30%	
Barnett and Reynolds	Ref. 7	10–1000		<10%			
Morgan *et al.*	Ref. 16	1.25–25				<5%	
Toburen *et al.*	Ref. 9	100–2500		<10%	<10%		
D'yachkov *et al.*	Ref. 17	10–400					−50%
σ_{0-}							
Williams	Ref. 11	2–50	−10%	−30%			
Stier and Barnett	Ref. 6	4–30	<5%	<5%			
Morgan *et al.*	Ref. 16					<10%	

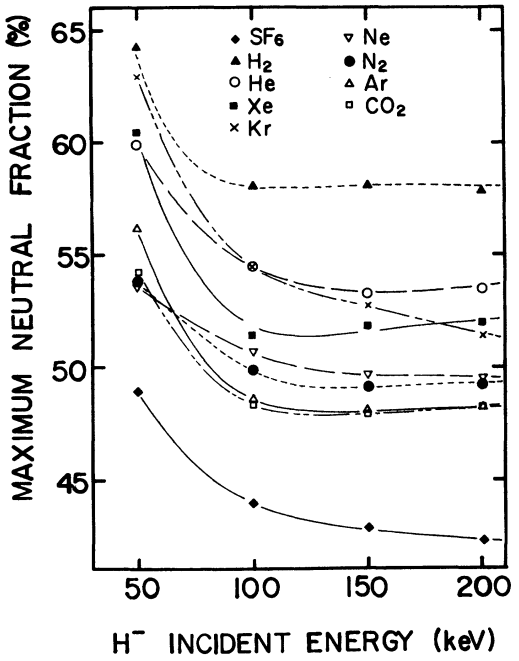

FIG. 8. F_0^{max} as a function of the energy for a variety of gas targets.

pared fast neutral beams by charge transfer with an H^+ ion beam incident. It seems reasonable that H^0 atoms in excited states are less probable if the fast neutral beam is prepared by stripping H^- ions than if it is prepared by charge transfer with H^+ ions incident.

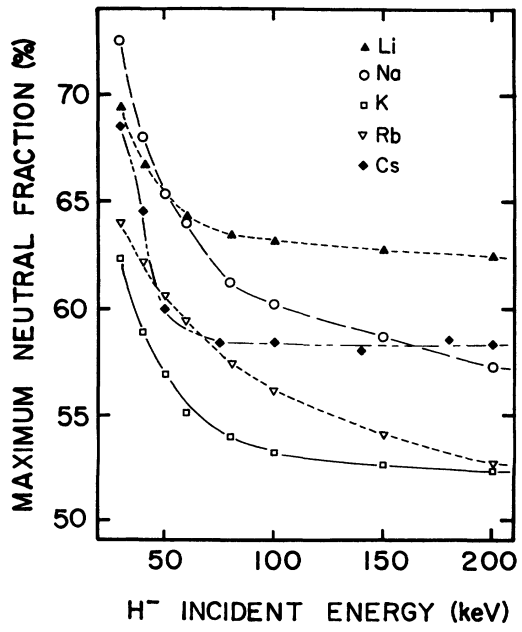

FIG. 9. F_0^{max} as a function of the energy for Li, Na, K, Rb, and Cs vapor targets.

TABLE X. Maximum neutral yield for a 100-keV H^- beam incident on various gases and vapors.

Gas or vapor	F_0^{max}
D_2	58.3 ± 1.0 %
O_2	49.3
Natural gas [a]	52.4
C_4H_{10}	48.6
C_5H_{12}	47.0
Br_2	48.7
I_2	48.9
CF_4	45.9 ± 1.0 %
CHF_3	47.2
$CClF_3$	44.3
$CBrF_3$	47.1
Water	50.9
Acetone	48.0
2-propanol	47.9

[a] 85–90 % methane by weight.

An interesting feature seen from our data is that the values of σ_{-0} are 2–10 times larger than σ_{+} for the same target for all the energies and targets investigated. This results from the fact that it is easier in a collision to strip the loosely bound (0.75 eV) electron from the H^- ion than the more tightly bound (13.6 eV) electron from the ground-state H^0 atom.

In the energy range 30–200 keV, σ_{-0} for H^- incident on an alkali atom is larger at all energies by a factor of 1.6–3.0 than σ_{-0} for H^- incident on the inert-gas atom with the same electron configuration as the alkali core. For example, σ_{-0} for H^- incident on Na is about 3 times larger than σ_{-0} for H^- incident on Ne at all energies in the range 30–200 keV.

In the energy range 30–200 keV the cross section σ_{-+} for H^- ions incident on a target has a simi-

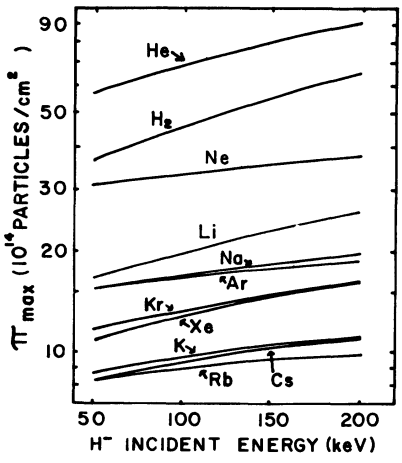

FIG. 10. π_{max} as a function of the energy for a variety of targets.

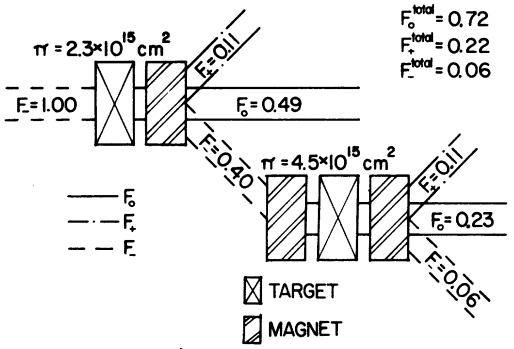

FIG. 11. A schematic diagram of a two target apparatus to increase the neutral yield.

lar energy dependence but is only 0.23–0.45 times as large as the cross section σ_{g+} for fast H(1s) atoms incident on the same target. This seems reasonable since in the first case both a loosely bound (0.75 eV) electron and a tightly bound (13.6 eV) electron are removed, where as in the latter case only one tightly bound (13.6 eV) electron is removed.

Another interesting feature of the data on σ_{-+} and σ_{g+} is the result that in the energy range 30–200 keV, the cross sections σ_{-+} and σ_{g+} for H^- ions or ground-state H^0 atoms incident on alkali atoms, are similar in value and in energy dependence as σ_{-+} and σ_{g+} for H^- ions or ground-state H^0 atoms incident on the inert gas that has the same electron configuration as the alkali core. For example, σ_{-+} for H^- incident on Na is almost the same as σ_{-+} for H^- incident on Ne, and σ_{g+} for fast H(1s) atoms incident on Na is almost the same as σ_{g+} for fast H(1s) atoms. Similar results hold for the other alkali-rare-gas targets. We speculate that this may indicate that the core of the alkali atom plays an important role in the cross sections σ_{-+} and σ_{g+}.

In the energy range 30–200 keV the data show that the values of σ_{g-} for H(1s) atoms incident on the alkali atoms are smaller in value and similar in energy dependence to σ_{g-} for H(1s) atoms incident on the inert gas that has the same electron configuration as the alkali core.

Calculations of the cross sections σ_{-0} and σ_{g+} for H^- ions and fast H(1s) atoms incident on He, Ne, Ar, Kr, and Xe targets in the energy range 30–200 keV have been carried out by Bates *et al.*[18-20] and by Dewangen and Walters[21] using the classical impulse model.

IV. MAXIMUM NEUTRAL YIELDS

We have measured the fractional yields of H^+ ions, H^- ions, and fast H^0 atoms when H^- ions are incident on a variety of targets. From the measured values of N_+, N_0, and N_- as functions of π we obtain F_-, F_0, and F_+ as functions of π. Figure 7 shows F_+, F_0, and F_- as functions of π for 100-keV H^- ions incident on a K vapor target. The neutral fraction F_0 increases from zero at $\pi=0$, reaches a maximum value of $F_0^{max}=0.532$ for $\pi = 1\times10^{15}$ atoms/cm^2, and then decreases to the equilibrium neutral fraction $F_0^{\infty}=0.14$ as π increases to a very large value. The behavior of F_0 as a function of π exhibited in Fig. 7 is typical of the behavior of all targets. For all targets studied the total transmission is greater than 99% at the maximum neutral yield. The measurement of the target thickness is not required in the determination of F_0^{max}. Thus the uncertainty in F_0^{max} results only from the uncertainties in N_+, N_0, and N_-. The uncertainty in F_0^{max} is estimated to be ±3%.

The maximum neutral fractions for 30–200-keV H^- ions incident on various gas and alkali vapor targets are plotted in Figs. 8 and 9. An interesting feature of these data is the insensitivity of F_0^{max} to energy in the range 100-200 keV. Table X contains F_0^{max} for 100-keV H^- ions incident on 14 other gases and vapors. The target thickness π_{max}, at which F_0 reaches its maximum value, is plotted in Fig. 10 as a function of the incident H^-

TABLE XI. Equilibrium negative fraction $\times10^5$, $F_-^{\infty}\times10^5$, for hydrogen incident on H_2, He, Ne, Ar, Kr, and Xe as a function of beam energy (keV).

Energy	H_2	He	Ne	Ar	Kr	Xe
30	1300 ± 130	940 ± 94	690 ± 69	435 ± 44	830 ± 83	800 ± 80
40	1050 ± 105	860 ± 86	465 ± 47	340 ± 34	640 ± 64	435 ± 44
50	730 ± 73	720 ± 72	360 ± 36	270 ± 27	500 ± 50	310 ± 31
60	480 ± 48	600 ± 60	280 ± 28	200 ± 20	340 ± 34	220 ± 22
80	190 ± 27	350 ± 40	180 ± 26	93 ± 13	155 ± 23	120 ± 18
100	68 ± 10	190 ± 26	110 ± 15	39 ± 6	56 ± 8	49 ± 7
150		43 ± 7				4.9 ± 0.7
200		9.0 ± 1.4				0.60 ± 0.1

TABLE XII. Equilibrium negative fraction $\times 10^5$, $F_-^\infty \times 10^5$, for hydrogen incident on Li, Na, K, and Rb as a function of beam energy (keV).

Energy (keV)	Li	Na	K	Rb
30	31.0 ± 3	66.0 ± 7	125 ± 13	230 ± 23
40	12.2 ± 1	35.0 ± 4	105 ± 11	210 ± 21
50	8.4 ± 0.9	25.0 ± 3	87.0 ± 9	183 ± 18
60	6.0 ± 0.8	18.0 ± 2	72.0 ± 7	135 ± 14
80	4.3 ± 0.8	14.0 ± 2	40.0 ± 4	58 ± 6
100	3.5 ± 0.7	11.0 ± 1	24.0 ± 3	25.0 ± 3
150		5.1 ± 0.8	4.2 ± 0.7	2.6 ± 0.5
200		2.5 ± 0.6	0.8 ± 0.2	

ion energy for 11 gas and vapor targets. The uncertainty in the measurements of π_{max} is about ±20%.

A noticeable trend in the measurements of F_0^{max} for H^- ions incident on molecular targets is the dependence of F_0^{max} on the number of atoms per molecule in the molecular target. The more atoms per molecule in the target the smaller is F_0^{max}. The inert gases and alkali vapors exhibit no such obvious correlations.

Our measurements of F_0^{max} for H^- incident on H_2 together with the measurements of Smythe and Toevs,[22] the measurements of Dimov and Dudnikov,[23] and a calculation of Berkner *et al.*[24] show that F_0^{max} is nearly constant for energies 100 keV to 14 MeV for H^- ions incident on a H_2 target. D'yachkov[25] has measured F_0^{max} for 100–400-keV H^- incident on Li, Mg, and Zn and found F_0^{max} to be constant with respect to energy.

Efficient neutralizers of 100-200-keV H^- ions are Li, H_2, and Cs with F_0^{max} of 0.63, 0.58, and 0.58, respectively. A larger yield of fast H^0 atoms can be obtained using two separate targets. Figure 11 shows a schematic drawing of an apparatus using two targets to neutralize 100-keV H^- ions incident on H_2 gas. The first target has a thickness that converts 49% of the H^- ions into H^0 atoms. The remaining H^- ions are deflected into a second target with a target thickness of π_{max}. A combined yield of 72% H^0 atoms can be obtained in this manner. The same two target scheme for 100-keV H^- ions incident on Li or Cs will result in neutral yields of 76.5% and 72%, respectively. The numerical values of the fractional yields from two targets are obtained from calculations similar to those described in Sec. VI of this paper.

V. EQUILIBRIUM FRACTIONS

At very large values of the target thickness the fractional yields become independent of the value of π. The value of the fractional yield for very large π is called the equilibrium fraction. We have measured the equilibrium fractions F_0^∞ and F_-^∞ for H^- ions incident on a variety of targets. Although we have used an incident H^- ion beam to measure the equilibrium fractions, the equilibrium fractions are independent of the charge composition of the incident beam. The methods used to measure the equilibrium fractions are similar to those described in Ref. 26. The transmission $T = (N_+ + N_0 + N_-)/N_s$ is typically only about 0.5 or less at equilibrium values of π, since particles are scattered out of the acceptance angle of the

TABLE XIII. Equilibrium neutral fraction F_0^∞ (%) for hydrogen incident on H_2, He, Ne, Ar, Kr, and Xe as a function of beam energy (keV).

Energy	H_2	He	Ne	Ar	Kr	Xe
30	73.5 ± 3.7	58.5 ± 3.0	44.5 ± 2.2	54.0 ± 2.7	63.4 ± 3.2	66.8 ± 3.3
40	63.5 ± 3.2	52.6 ± 2.6	37.6 ± 1.9	46.5 ± 2.3	56.0 ± 2.8	54.5 ± 2.7
50	53.5 ± 2.7	48.5 ± 2.4	33.9 ± 1.7	40.4 ± 2.0	50.2 ± 2.5	44.5 ± 2.2
60	44.0 ± 2.2	43.1 ± 2.2	30.5 ± 1.5	34.5 ± 1.7	43.0 ± 2.2	35.5 ± 1.8
80	30.0 ± 1.5	33.5 ± 1.7	25.0 ± 1.3	24.2 ± 1.2	30.9 ± 1.5	23.2 ± 1.2
100	19.2 ± 1.0	25.2 ± 1.3	20.8 ± 1.0	16.5 ± 0.8	20.1 ± 1.0	15.0 ± 0.8
150	6.3 ± 0.5	12.7 ± 0.8	12.3 ± 0.8	6.0 ± 0.5	6.2 ± 0.5	5.4 ± 0.5
200	2.1 ± 0.2	6.6 ± 0.5	6.9 ± 0.6	2.8 ± 0.3	2.0 ± 0.2	2.7 ± 0.3

TABLE XIV. Equilibrium neutral fraction F_0^∞ (%) for hydrogen incident on Li, Na, K, Rb, and Cs as a function of beam energy (keV).

Energy	Li	Na	K	Rb	Cs
30	18.6 ± 1.0	28.5 ± 1.5	30.7 ± 1.5	41.0 ± 2.0	54.0 ± 2.0
40	12.0 ± 1.0	19.3 ± 1.0	27.5 ± 1.5	37.1 ± 2.0	45.0 ± 2.0
50	9.2 ± 0.5	15.6 ± 1.0	24.5 ± 1.5	34.1 ± 1.5	37.5 ± 1.5
60	7.8 ± 0.5	12.5 ± 1.0	21.7 ± 1.0	30.1 ± 1.5	
75					27.0 ± 2.0
80	6.6 ± 0.5	10.2 ± 1.0	17.2 ± 1.0	21.3 ± 1.0	
100	5.6 ± 0.5	9.0 ± 0.5	13.0 ± 1.0	15.0 ± 1.0	15.0 ± 1.0
140					7.5 ± 1.0
150	3.5 ± 0.3	6.7 ± 0.6	5.8 ± 0.5	6.2 ± 0.5	
200	2.5 ± 0.3	4.9 ± 0.6	2.8 ± 0.3	2.0 ± 0.3	2.6 ± 0.3

detectors. For equilibrium values of π each particle in the beam has changed its charge many times before it emerges from the target, and hence, the angular distributions of the H^+, H^0, and H^- beams are the same. We have attempted to ensure that the equilibrium fractions we measure are independent of the transmission as follows. Each detector subtends the same angle, about 1.50°, as seen from the center of the target so that each detector intercepts the same fraction of its beam. Before measurement of the equilibrium fraction the beam is carefully aligned so that each component of the beam is centered on its detector. The ions emerging from the target are deflected by only 4° which results in negligible focusing. As a result of the attention to these considerations we believe that the uncertainty in the measurements is relatively small. The uncertainty in most of the equilibrium fraction measurements is estimated to be 4–7%. This uncertainty is primarily due to a slight misalignment of the apparatus added to error in the beam measurements. The uncertainty when the equilibrium fractions are less than 0.05 is 7–20%. This larger uncertainty is primarily due to random scatter in the measurement of the small current.

The measured equilibrium fractions F_-^∞ and F_0^∞ for 30–200-keV H^- ions incident on H_2, He, Ne, Ar, Kr, Xe, Li, Na, K, Rb, and Cs are tabulated in Tables XI–XIV and some of the data are plotted in Figs. 12 and 13. Stier and Barnett[6] have reported values of F_0^∞ for H_2, He, Ne, and Ar that are in good agreement with our values of F_0^∞. Il'in *et al.*[27] have reported values of F_0^∞ for Na that are in agreement with our values. However, D'yachkov *et al.*[28] have reported values of F_0^∞ for Na and Li that are almost a factor of 2 below our measurements.

An interesting feature of the data is the result that the energy dependence of F_0^∞ is similar for

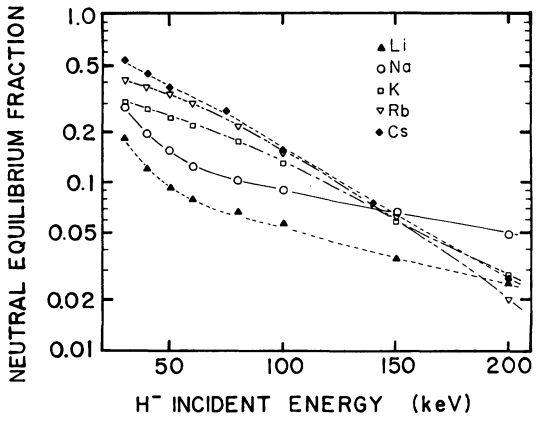

FIG. 12. F_0^∞ as a function of the energy for Li, Na, K, Rb, and Cs vapor targets.

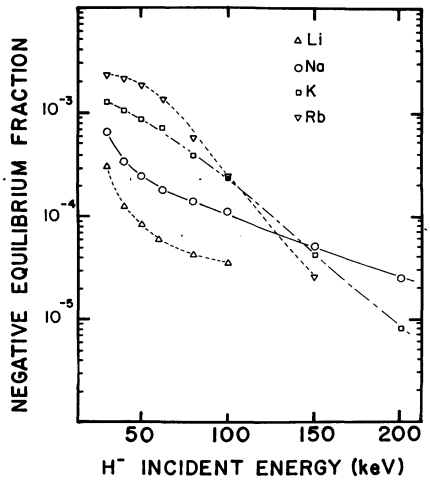

FIG. 13. F_-^∞ as a function of the energy for Li, Na, K, and Rb vapor targets.

30–200 keV H^- ions incident on an alkali vapor or the inert gas that has the same electron configuration as the alkali core. A possible explanation for this feature is the following. The neutral equilibrium fractions in the energy range 30–200 keV are primarily determined by the cross sections σ_{g+} and σ_{+0}. Il'in *et al.*[27] and Meyer *et al.*[29] speculate that the cross section σ_{+0} for H^+ ions with energies above 30 keV incident on an alkali atom is primarily determined by the core electrons in the alkali atom. We speculate that the cross section σ_{g+} for a 20–200 keV H(1s) atom incident on an alkali atom is primarily determined by the alkali core. If both of these speculations are correct then F_0^∞ will have the same energy dependence for an alkali vapor and for the inert gas that has the same electron configuration as the alkali core. Li and He are exceptions since the He-like core in Li is much smaller than the He atom.

Another interesting feature of the data is the result that the values of F_-^∞ are larger for 30–200-keV H^- ions incident on the inert gases than the corresponding alkali metals. An explanation for this based on the measured cross section follows. The primary cross section for producing H^- ions, σ_{g-}, is larger for the inert gases than for the alkali vapors. The primary cross section for destroying H^- ions, σ_{-0}, is larger for the alkali vapors than the inert gases. Therefore, the overall effect is that the negative equilibrium fraction, is larger for the inert gases than the alkali vapors.

VI. NEUTRALIZATION PROCESS

We have calculated F_+, F_0, and F_- as a function of π for 30–200 keV H^- incident on Ne, Ar, Kr, Xe, Li, Na, K, Rb, and Cs using a three-charge-component model by solving the following differential equations:

$$\frac{dF_+}{d\pi} = -(\sigma_{+0} + \sigma_{+-})F_+ + \sigma_{g+}F_0 + \sigma_{-+}F_- ,$$

$$\frac{dF_0}{d\pi} = \sigma_{+0}F_+ - (\sigma_{g+} + \sigma_{g-})F_0 + \sigma_{-0}F_- ,$$

$$\frac{dF_-}{d\pi} = \sigma_{+-}F_+ + \sigma_{g-}F_0 - (\sigma_{-+} + \sigma_{-0})F_- .$$

From the calculated values of F_0 as a function of π we obtain a calculated value of F_0^{max} and F_0^∞. In solving the three simultaneous differential equations we use the measured values of σ_{+0},[27,29,30,31] σ_{-+}, σ_{-0}, and σ_{g+}. In the energy range 30–200 keV the cross sections σ_{g-} and σ_{+-} are very small and have a negligible effect on the calculation of F_0^{max} and F_0^∞. They are set equal to zero. The calculated and measured values of F_0^{max} for 30–200-keV H^- ions incident on Ne, Ar, Kr, Xe, Li, Na, K, Rb, and Cs are in good agreement. Above 100 keV F_0^{max} is determined primarily by the cross sections σ_{-0}, σ_{g+}, and σ_{-+}. The values of F_0^{max} become almost constant with respect to energy above 100 keV because σ_{-0}, σ_{g+}, and σ_{-+} have similar energy dependence above 100 keV.

The various cross sections for 30–200 keV deuterium and hydrogen incident at the same velocity on a given target are the same. Thus the maximum neutral fractions for H^- and D^- incident at the same velocity on a given target are equal.

The calculated and measured values of F_0^∞ for 30–200 keV H^- ions incident on Ne, Ar, Kr, Xe, Li, Na, K, Rb, and Cs are not all in good agreement. The measured values of F_0^∞ for the alkali vapors are about 15–30% below the calculated values of F_0^∞. The measured values of F_0^∞ for the inert gases are 0–15% below the calculated values.

Figure 7 shows that for H^- ions incident on K the experimental and calculated values of F_0 are in good agreement for values of π less than 10^{15} atoms/cm^2, but that for values of π near equilibrium the calculated values of F_0^∞ are somewhat higher than the experimental values. The cross section σ_{g+} used in the calculation is the cross section for ionization of a ground-state H^0 atom. The results indicate that at low values of π the H^0 atoms are produced primarily in the ground state as a result of stripping an electron from H^-, and hence, the calculated values of F_0 agree well with experiment. As π increases above π_{max} a significant fraction of the H^0 atoms are in excited states. The excited H^0 atoms are produced either by H^+ ions capturing an electron into an excited state or by collisional excitation of ground-state H^0 atoms. A H^0 atom in an excited state has a larger cross section for ionization than a H^0 atom in the ground state. At large values of π, the average cross section for ionizing the H^0 atoms is therefore larger than σ_{g+}. The average cross section for ionization is obtained by averaging over the distribution of ground-state and excited-state H^0 atoms. Therefore, the calculated values of F_0^∞ calculated using σ_{g+} in the three-component model are higher than the measured values of F_0^∞.

ACKNOWLEDGMENTS

We acknowledge the partial support of this research by the United States Department of Energy. We also acknowledge Brynn Anderson for help in reducing the data.

*Now at IBM Watson Research Center, P.O. Box 218, Yorktown Heights, N.Y. 10598.

[1]R. Hultgren, P. D. Desai, D. T. Hawkins, M. Gleiser, K. K. Kelley, and D. D. Wagman, *Selected Values of the Thermodynamic Properties of the Elements* (American Society for Metals, Cleveland, 1973).

[2]K. H. Berkner, B. R. Meyers, and R. V. Pyle, Rev. Sci. Instrum. 39, 1204 (1968).

[3]M. W. Geis, K. A. Smith, and R. D. Rundel, J. Phys. E 8, 1011 (1975).

[4]R. J. Girnius, C. J. Anderson, and L. W. Anderson, Phys. Rev. A 16, 2225 (1977).

[5]Atomic Data for Controlled Fusion Research, Report No. ORNL-5206, 1977 (unpublished).

[6]P. M. Stier and C. F. Barnett, Phys. Rev. 103, 896 (1956).

[7]C. F. Barnett and H. K. Reynolds, Phys. Rev. 109, 355 (1958).

[8]E. S. Solov'ev, R. N. Il'in, V. A. Oparin, and N. V. Fedorenko, Zh. Eksp. Teor. Fiz. 42, 659 (1962) [Sov. Phys.-JETP 15, 459 (1962)].

[9]L. H. Toburen, M. Y. Nakai, and R. A. Langley, Phys. Rev. 171, 114 (1968).

[10]J. Heinemeier, P. Hvelplund, and F. R. Simpson, J. Phys. B 9, 2669 (1976).

[11]J. F. Williams, Phys. Rev. 153, 116 (1967).

[12]J. F. Williams, Phys. Rev. 154, 9 (1967).

[13]Ia. M. Fogel', V. A. Ankudinov, and R. E. Slabospitskii, Zh. Eksp. Teor. Fiz. 32, 453 (1957) [Sov. Phys.-JETP 5, 382 (1957)].

[14]Ia. M. Fogel', V. A. Ankudinov, D. V. Pilipenko, and N. V. Topolia, Zh. Eksp. Teor. Fiz. 34, 579 (1958) [Soviet Phys.-JETP 7, 400 (1958)].

[15]J. B. H. Stedeford and J. B. Hasted, Proc. R. Soc. London Ser. A 227, 466 (1955).

[16]T. J. Morgan, K. H. Berkner, W. G. Graham, R. V. Pyle, and J. W. Stearns, Phys. Rev. 14, 664 (1976).

[17]B. A. D'yachkov, Sov. At. Energy 27, 958 (1969).

[18]D. R. Bates and J. C. G. Walker, Planet. Space Sci. 14, 1367 (1966).

[19]D. R. Bates and J. C. G. Walker, Proc. Phys. Soc. 90, 333 (1967).

[20]D. R. Bates, V. Dose, and V. A. Young, J. Phys. B 2, 930 (1969).

[21]D. P. Dewangen and H. R. J. Walters, J. Phys. B 11, 3983 (1978).

[22]R. Smythe and J. W. Toevs, Phys. Rev. 139, A15 (1965).

[23]G. I. Dimov and V. G. Dudnikov, Zh. Tekh. Fiz. 36, 1239 (1966) [Sov. Phys.-Tech. Phys. 11, 919 (1967)].

[24]K. H. Berkner, R. V. Pyle, and J. W. Stearns, Nucl. Fusion 15, 249 (1975).

[25]B. A. D'yachkov, Tech. Phys. U.S.S.R. 13, 1036 (1969).

[26]R. J. Girnius, L. W. Anderson, and E. Staab, Nucl. Instrum. Methods 143, 505 (1977).

[27]R. N. Il'in, V. A. Oparin, E. S. Solov'ev, and N. V. Fedorenko, Zh. Tekh. Fiz. 36, 1241 (1965) [Sov. Phys.-Tech. Phys. 11, 921 (1967)].

[28]B. A. D'yachkov and V. I. Zinenko, Sov. At. Energy 24, 16 (1968).

[29]F. W. Meyer, C. J. Anderson, and L. W. Anderson, Phys. Rev. A 15, 455 (1977).

[30]F. J. de Heer, J. Schutten, and H. Moustafa, Physica (Netherlands) 32, 1766 (1966).

[31]V. V. Afrosimov, R. N. Il'in, and E. S. Solov'ev Zh. Tekh. Fiz. 30, 705 (1960) [Sov. Phys.-Tech. Phys. 5, 661 (1960)].